# Electrochemical study on effect of Au, Ag, Pd and Pt on corrosion behaviour of $Fe_3Al$ in molten NaCl–KCl

**G. Salinas[1], J. G. Gonzalez-Rodriguez*[1], J. Porcayo-Calderon[1], V. M. Salinas-Bravo[2], G. Lara-Rodriguez[3] and A. Martinez-Villafañe[4]**

The corrosion behaviour of $Fe_3Al$ intermetallic alloyed with 1 at-%Ag, Au, Pt and Pd in NaCl–KCl (1 : 1M) at 700°C, typical of waste gasification environments, has been evaluated using polarisation curves, linear polarisation resistance and electrochemical impedance spectroscopy measurements and compared with an Ni based alloy, namely Inconel 600. Results have shown that, for short testing times, the addition of noble elements increased the corrosion rate for base $Fe_3Al$ intermetallic alloy, but it was decreased for long testing times by forming a protective corrosion product layer. Additionally, base $Fe_3Al$ intermetallic alloy had higher corrosion rates than Inconel 600.

**Keywords:** $Fe_3Al$, Hot corrosion, Electrochemical impedance

## Introduction

Iron aluminides have been considered to be used as structural materials due to their improved resistance at high temperatures into oxidising environments. Iron aluminides based around the compositions $Fe_3Al$ and FeAl are candidates for high temperature materials because of their excellent oxidation resistance, relatively low cost and material density.[1–3] Structural materials used in the construction of boiler or supercritical steam turbines, or waste incinerators and biomass fired boilers[4,5] are exposed to temperatures between 600 and 700°C, under pressure and corrosive environments such as molten salts. Problems with process equipment resulting from fireside corrosion have been frequently encountered in incinerators. The major problem is the complex nature of the feed (waste) as well as corrosive impurities that form low melting point compounds with heavy and alkali metal chlorides that prevent the formation of protective oxide scales and then cause an accelerated degradation of metallic elements.[4] The effects of NaCl, KCl and their mixtures with sulphates have been studied in detail so far;[5–11] however, very few of them have been carried out using electrochemical techniques, but these techniques have been applied in some other different systems.[12–21] Thus, Aung used potentiodynamic polarisation curves, electrochemical noise and electrochemical impedance spectroscopy (EIS) in a high temperature sensor for *in situ* monitoring of hot corrosion.[12] The corrosion of bipolar plate and current collector materials in molten carbonate fuel cells was investigated by Zhu *et al.*[13] using Tafel extrapolation, linear polarisation resistance, chronopotentiometry and EIS to determine corrosion rates of iron and iron based alloys in molten carbonate melts for both cathode and anode molten carbonate fuel cells environments. During the initial stages, agreement among the methods was good but could have differed after a corrosion layer formed on the surface. In another study, Ducati *et al.*[16] showed in one of the earliest works on this topic. Zeng *et al.* used EIS studies for the corrosion of two-phase Cu–15Al alloy in the eutectic $(Li,K)_2CO_3$ at 650°C[14] and for $Ni_3Al$ alloy in (Li, Na, K)$_2SO_4$ at 650°C.[17] They found that the complex plane of the electrochemical impedance suggested that the fast corrosion rate of these alloys was due to the formation of a non-protective oxide and that the corrosion process was controlled by the diffusion of oxidants. Barraza-Fierro and co-workers[19] have successfully used electrochemical techniques to study the effect of Li and Cu addition to base intermetallic Fe–40 at-%Al on the corrosion behaviour in molten LiCl–55 wt-%KCl eutectic salt at 450, 500 and 550°C.

It is well known that noble elements such as Ag, Au, Pt, etc. can form cathodic sites when added as alloying elements to engineering structural materials, but there is very little information regarding their effects on the corrosion performance of engineering materials in molten salts. Regarding low temperature corrosion, the effect of noble elements when added to stainless steels in sulphuric acid, Peled *et al.*[22] found that additions of Ag improved the corrosion resistance and remained as inclusions,

[1]Universidad Autónoma del Estado de Morelos, CIICAP, Avenida Universidad 1001, Colonia Chamilpa, Cuernavaca, Morelos 62500, Mexico
[2]IIE, Gerencia de Procesos Térmicos, Avenida Reforma 120, Temixco, Morelos, Mexico
[3]Universidad Nacional Autonoma de Mexico, Instituto de Investigaciones en Materiales, Circuito Exterior S/N, Cd. Universitaria, Mexico DF C.P. 04510, Mexico
[4]Centro de Inv. En Materiales Avanzados, Miguel de Cervantes 120, Complejo Industrial Chihuahua, Chihuahua C.P. 31109, Mexico

*Corresponding author, email ggonzalez@uaem.mx


Published by Maney on behalf of the Institute
Received 18 April 2013; accepted 7 January 2014
DOI 10.1179/1743278214Y.0000000150

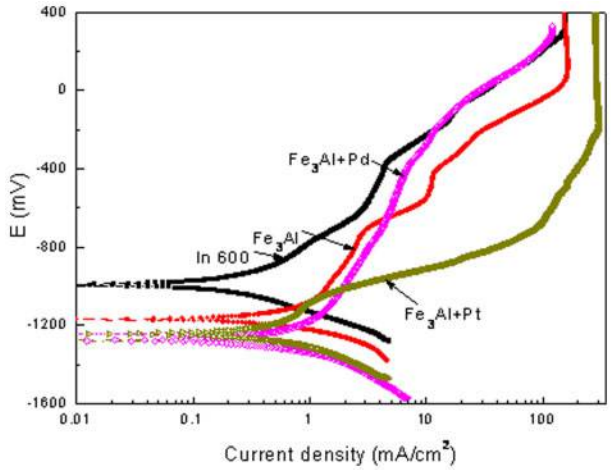


**1 Effect of Pd and Pt in polarisation curves of $F_3Al$ intermetallic alloy in NaCl–KCl (1 : 1M) at 700°C**

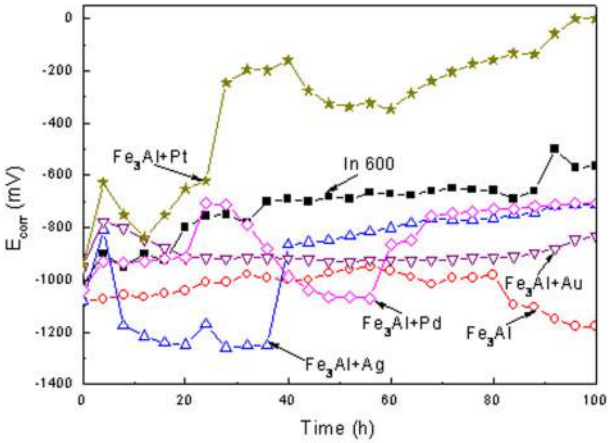


**3 Change of $E_{corr}$ value with time for $F_3Al$ intermetallic alloyed with Au, Ag, Pd and Pt in NaCl–KCl (1 : 1M) at 700°C**

whereas additions of up to 2 wt-% were sufficient to preserve the passive state, but higher contents result in a high tendency for breakdown of the passive layer due to very high cathodic activity when Ag, Au, Pd or Pt was added.[23] With respect to the molten salt corrosion, Janz *et al.*[24,25] evaluated the corrosion of gold–palladium, nickel, platinum, silver, gold and 347 type stainless steel in molten alkali carbonates at 600–900°C, finding little or negligible corrosion of noble elements, whereas 347 type stainless steel was found highly resistant to attack. Some other researchers have studied the effect of noble elements in the oxidation behaviour[26,27] or sulphidation performance of structural materials,[28,29] but not in molten salts. Thus, the aim of the present work was to study the effect of noble elements in the corrosion behaviour of $Fe_3Al$ intermetallic in molten NaCl–KCl salts using electrochemical techniques.

## Experimental

The material used here was $Fe_3Al$ intermetallic with additions of 1 at-%Ag, Au, Pd and Pt. Intermetallic alloys with a nominal composition of Fe+24Al+1*M*, where *M*=Ag, Au, Pd and Pt, were melted in an induction furnace using quartz crucibles under an argon atmosphere. All elements were of 99·9% purity. Specimens measuring 10 mm width, 5 mm height and 3 mm thickness were prepared. The working salt consisted of 500 mg $cm^{-2}$ of a eutectic mixture of NaCl–KCl, 1 : 1M, analytical grade for each test. The testing temperature was 700°C in static air condition. Before the tests, the specimens' surfaces were prepared by the standard technique of grinding with SiC from 240 to 600 grit emery paper, washed with water and degreased with acetone. For comparison, the same tests were carried out with a commercial nickel base alloy, namely Inconel 600. Electrochemical techniques included potentiodynamic polarisation curves, linear polarisation resistance (LPR) and EIS measurements. Details of the experimental set-up for the electrochemical cell used in this work are given elsewhere.[21] The body of the cell was a 15 mL silica crucible. The most important elements were reference and auxiliary electrodes made of a 0·5 mm diameter platinum (Pt) wire inside a mullite tube and filled with commercial refractory, ceramic cement. The electrical contact was made by welding an 80 wt-%Cr–20Ni wire to the specimen. Polarisation curves were obtained by polarising the specimens from −500 to +1500 $mV_{Pt}$ with respect to the free corrosion potential value $E_{corr}$ at a scanning rate of 1·0 mV $s^{-1}$. The LPR measurements were carried out by polarising the specimen from –10 to +10 mV with respect to $E_{corr}$, at a scanning rate of 1 mV $s^{-1}$ every

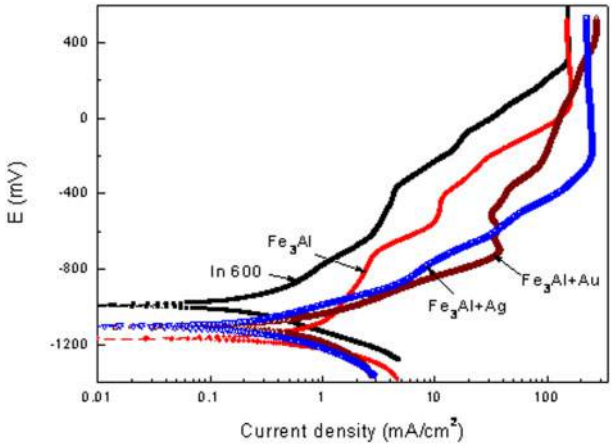


**2 Effect of Ag and Au in polarisation curves of $F_3Al$ intermetallic alloy in NaCl–KCl (1 : 1M) at 700°C**

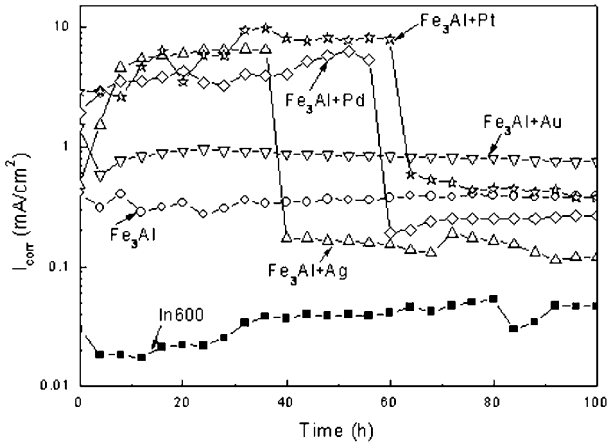


**4 Change of $I_{corr}$ value with time for $F_3Al$ intermetallic alloyed with Au, Ag, Pd and Pt in NaCl–KCl (1 : 1M) at 700°C**

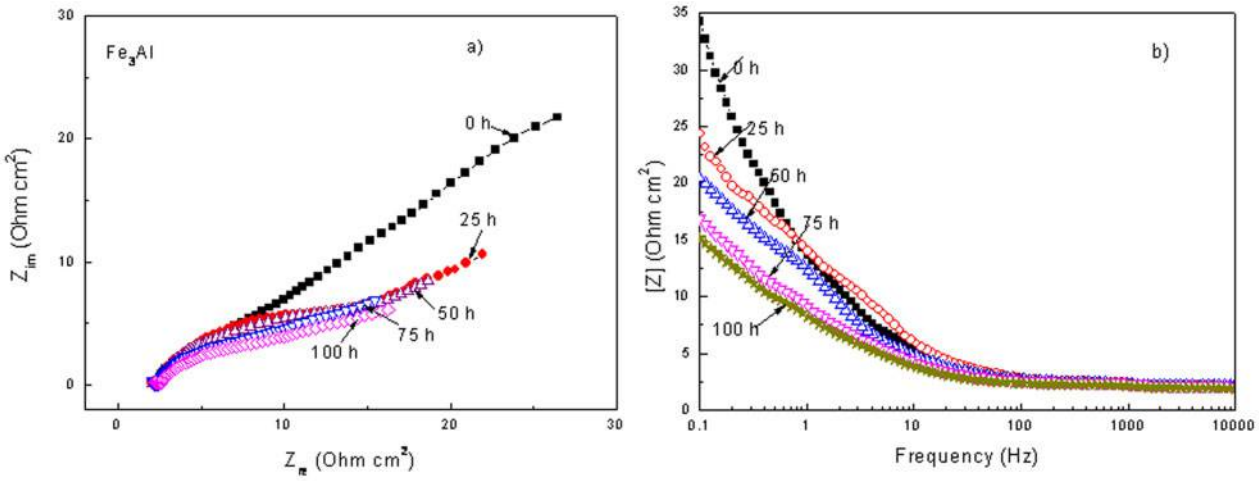


**5 Electrochemical impedance spectroscopy data in *a* Nyquist and *b* Bode format for $Fe_3Al$ intermetallic alloy in NaCl–KCl (1 : 1M) at 700°C**

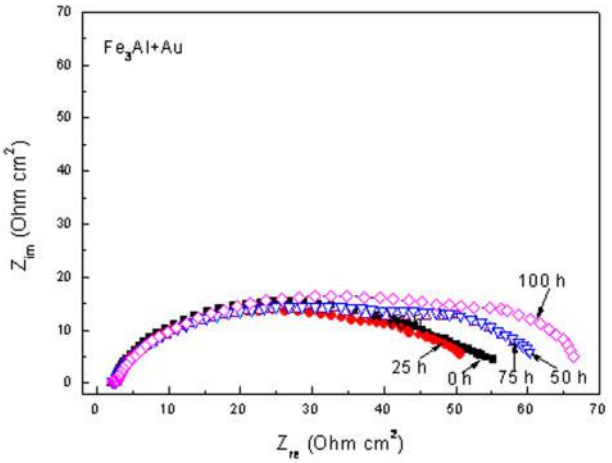


**6 Nyquist diagram for $Fe_3Al+Au$ intermetallic alloy in NaCl–KCl (1 : 1M) at 700°C**

4 h during 100 h. The original potential–current plots used to calculate the $R_p$ values are not reported here, but they followed a straight line trend. The EIS measurements were carried out in the frequency interval of 0·05 to 30 000 Hz at the $E_{corr}$ value using a PC4-300 Gamry potentiostat. The amplitude of the input sine wave voltage was 10 mV as recommended by previous works performed on this topic. One of each specimen was mounted in bakellite in cross-section and polished to analyse the subsurface corrosive attack using a scanning electron microscopy aided with energy dispersive spectroscopy to carry out microchemical analysis.

**Table 1 Tafel slopes for the different tested alloys in NaCl-KCl (1:1 M) at 700°C**

| Alloy | $\beta_a$ (mV/dec) | $\beta_c$ (mV/dec) |
|---|---|---|
| In 600 | 102 | 80 |
| $Fe_3Al$ | 76 | 58 |
| $Fe_3Al+Ag$ | 90 | 138 |
| $Fe_3Al+Au$ | 85 | 275 |
| $Fe_3Al+Pd$ | 125 | 300 |
| $Fe_3Al+Pt$ | 160 | 310 |

## Results and discussion

The effects of the addition of different noble elements in the polarisation curves for the $Fe_3Al$ intermetallic alloy in NaCl–KCl at 700°C together with that for Inconel 600 are shown in Figs. 1 and 2. It can be seen that all the alloys showed an active behaviour without evidence of a passive layer, with an anodic limiting current density or plateau at intermediate potentials, which is likely a salt fim due to the high dissolution rates, and another plateau at high anodic overpotentials due to mass transport limited control dissolution. Nickel base alloy Inconel 600 showed the noblest $E_{corr}$ value, whereas the most active was for the alloy containing Pd. In addition, the lowest anodic current density value was shown by Ni based alloy Inconel 600, and the highest value was exhibited by the $Fe_3Al+Pt$ alloy. It is clear that the anodic current density values for the base $Fe_3Al$ alloy increases when all the noble elements are added, showing a detrimental effect on them. The way that the anodic current density changed with the applied anodic potential for unalloyed $Fe_3Al$ and $Fe_3Al+Pd$ alloys was slower than the rest of the alloys containing either Au, Ag or Pt, indicating a lower dissolution rate for the formers, probably due to the type of corrosion products formed on their surfaces. Table 1 shows the Tafel slopes for all the tested alloys, where it can be seen that alloying elements increased both anodic and cathodic slopes, but this effect was much more pronounced for the cathodic slope, especially for Pd and Pt, which could be due to a very high cathodic activity when Ag, Au, Pd or Pt was added as established by Peled.[23]

The change in the $E_{corr}$ value with time for the different alloys in NaCl–KCl at 700°C is shown in Fig. 3, where it can be seen that after 30 h or so, all the $Fe_3Al$ alloys, except the one containing Pt, showed more active potential values than that for Inconel 600, whereas the alloy containing Pt showed nobler potential values than those for the Ni based alloy. Unalloyed $Fe_3Al$ and $Fe_3Al+Au$ alloys showed $E_{corr}$ values that are very stable with time, indicating corrosion products more or less stable, whereas those alloys containing either Ag or Pd reaching nobler values than unalloyed $Fe_3Al$ alloy towards the end of the test. The $E_{corr}$ value

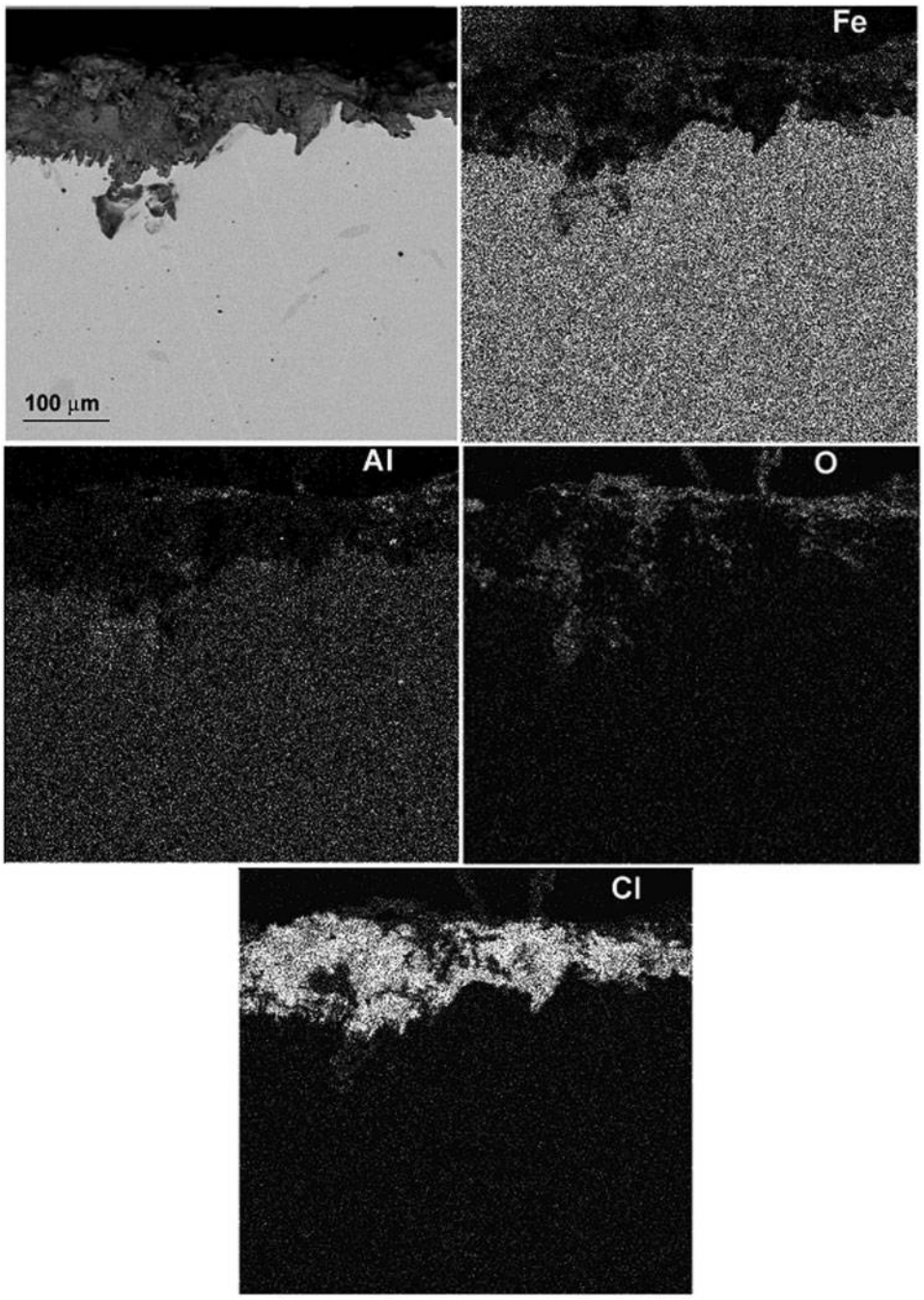


**7 Micrograph of $Fe_3Al$ intermetallic alloy corroded in NaCl–KCl (1 : 1M) at 700°C together with X-ray mappings of Fe, Al, O and Cl**

for the alloy containing Pt shifted towards very noble values during the whole testing time, indicating a very protective film formed by the corrosion products.

In order to study the change in the corrosion rate with time for the different alloys, some LPR measurements were performed and the $R_p$ values were converted into corrosion current density values $I_{corr}$ using the Stern–Geary equation and Tafel values given in Table 1. The change in the $I_{corr}$ value with time for the different alloys exposed to NaCl–KCl at 700°C during 100 h is shown in Fig. 4. The lowest $I_{corr}$ values were shown by Inconel 600 and unalloyed $Fe_3Al$ followed by the $Fe_3Al+Au$ alloy, at least during the first 40 h or so. On the other hand, the highest corrosion rates were exhibited for the alloy containing Ag, Pd and Pd, but after 40 h or so, the $I_{corr}$ values for these alloys decreased drastically reaching similar or even lower values than unalloyed $Fe_3Al$ alloys. Towards the end of the test, the unalloyed $Fe_3Al+Au$ alloy displayed the highest corrosion rate, but is very stable throughout time, indicating the stability of the formed corrosion products. The corrosion rate for Inconel 600 was very stable with time also, almost four times lower than the rest of the alloys.

Nyquist diagrams for unalloyed $Fe_3Al$ intermetallic (Fig. 5*a*) Nyquist data displayed a semicircle at high frequency values and a second semicircle at lower and intermediate frequencies at the beginning of the experiment. After 25 h of testing, the EIS data exhibited a semicircle at high frequency values followed by a 45° straight line at lower frequencies. This behaviour is typical of a process that is under a diffusion control, diffusion of aggressive ions through the scale; the

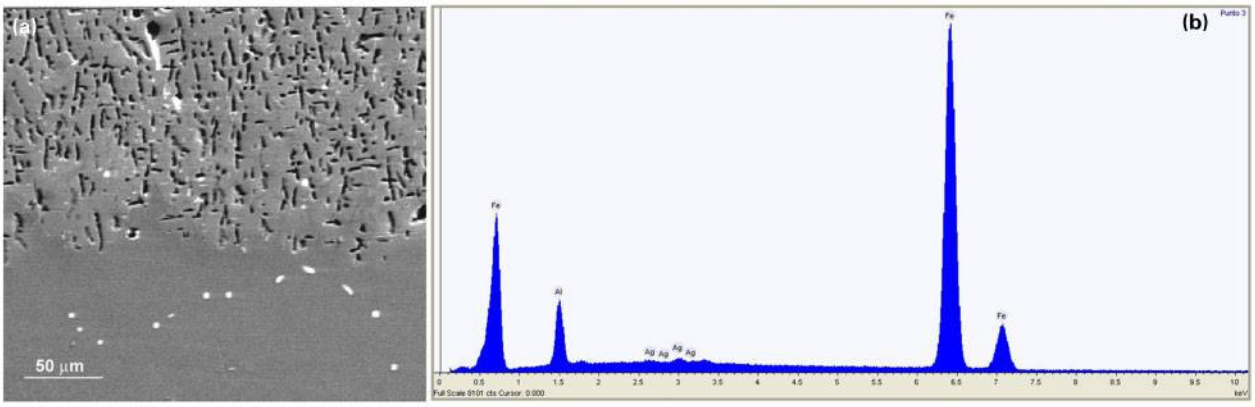


**8 Micrograph of corroded $Fe_3Al+Ag$ alloy together with chemical microanalysis of surface**

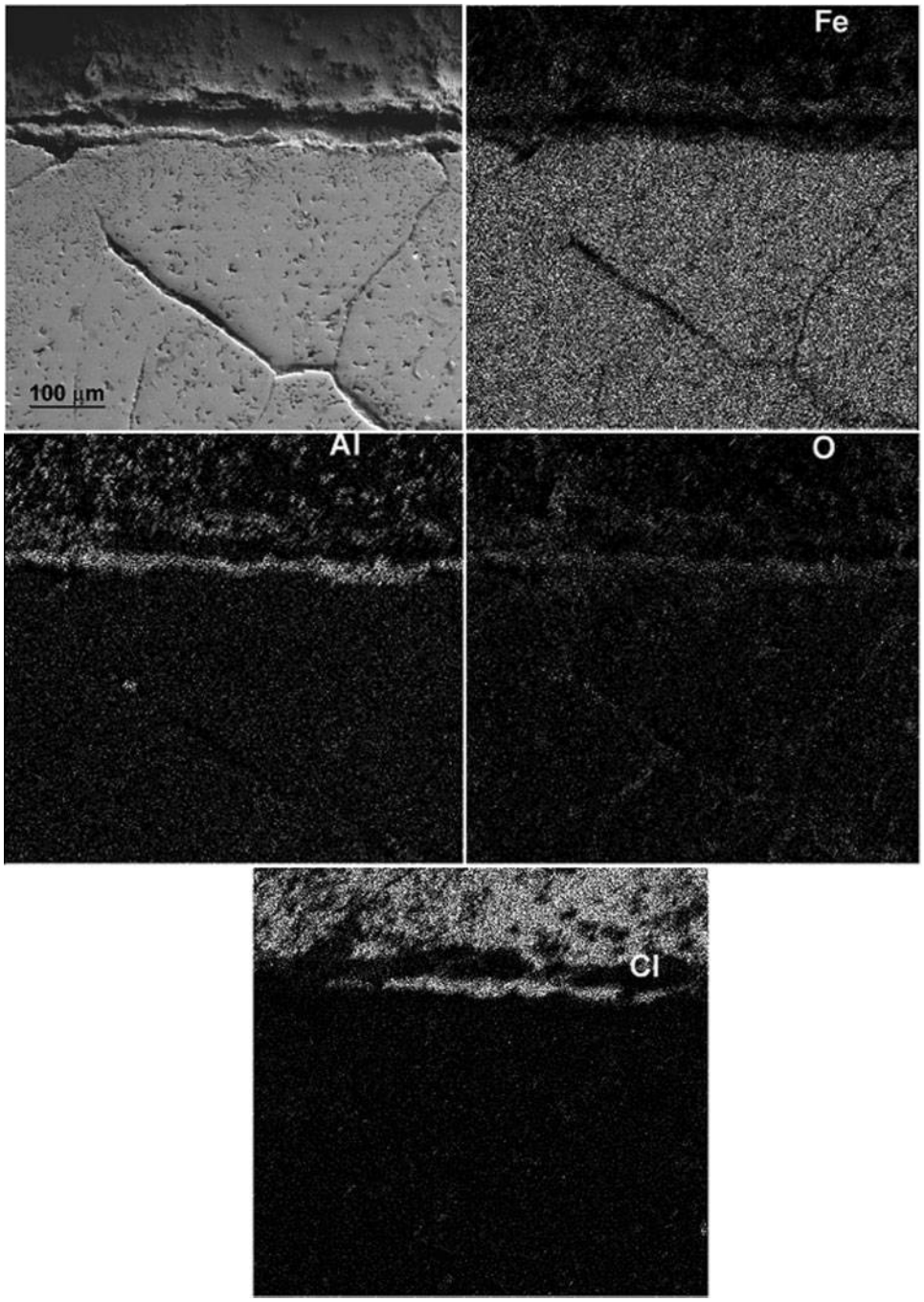


**9 Micrograph of $Fe_3Al+Ag$ intermetallic alloy corroded in NaCl–KCl (1 : 1M) at 700°C together with X-ray mappings of Fe, Al, O and Cl**

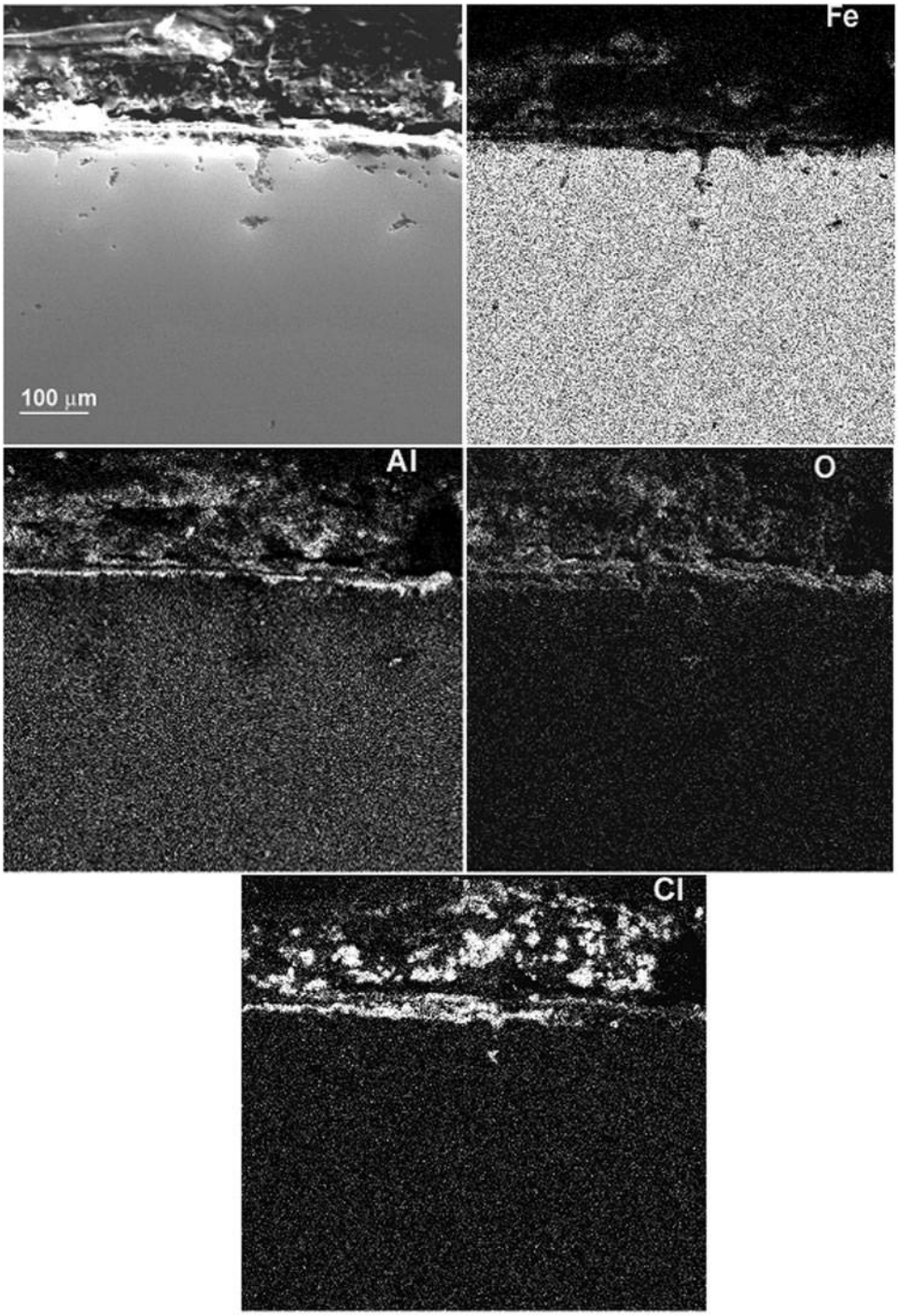


**10 Micrograph of $Fe_3Al+Pd$ intermetallic alloy corroded in NaCl–KCl (1 : 1M) at 700°C together with X-ray mappings of Fe, Al, O and Cl**

diameter of the high frequency semicircle remained more or less constant but much lower than that for the low frequency semicircle. Bode diagram for this alloy (Fig. 5*b*) clearly shows that the total impedance decreases as time increases, indicating an increase in the corrosion rate, just like the $I_{corr}$ result for this alloy shown in Fig. 4.

When Au is added, the behaviour was different to that exhibited by the base $Fe_3Al$ alloy (Fig. 6), since this time, Nyquist data displayed a single capacitive-like semicircle with its centre in the real axis at 0 and 25 h, indicating a corrosion process controlled by the charge transfer from the alloy to the electrolyte through the double electrochemical layer; however, for times longer than 50 h, the data display one semicircle at high and intermediate frequency values followed by a second semicircle at lower frequency values. The first semicircle is related with the charge transfer reaction, whereas the second semicircle is related with a formed, more or less, protective external layer. The total impedance increases slightly as time increases, opposite to the $I_{corr}$ behaviour shown by this alloy in Fig. 4, indicating a corrosion rate more or less constant with time.

A micrograph of corroded base $Fe_3Al$ alloy together with the X-ray mappings of Fe, Al, O and Cl is shown in Fig. 7. It can be seen that the corrosion products consist

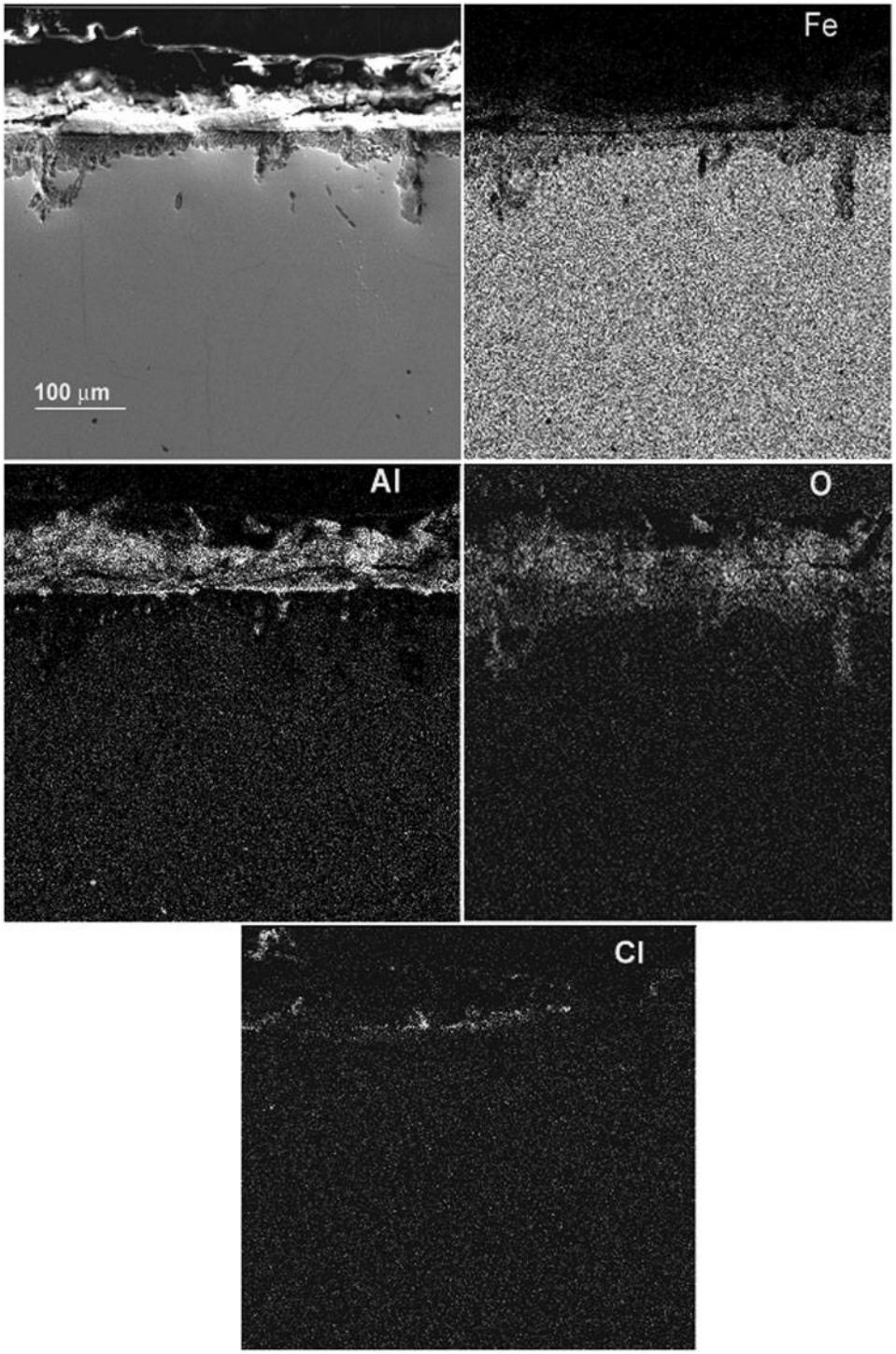


**11 Micrograph of $Fe_3Al+Pt$ intermetallic alloy corroded in NaCl–KCl (1 : 1M) at 700°C together with X-ray mappings of Fe, Al, O and Cl**

basically of iron and aluminium oxides that have been dissolved by chlorides. No evidence of internal attack by either oxygen or chloride is found, but only external damage in some cases taking place as localised, pitting-like corrosion. The alloy containing Ag (Fig. 8) suffered from localised type of corrosion around the silver particles, indicating that silver particles acted as cathodes and the surrounding matrix as anodes inducing a high cathodic activity as reported previously by Peled.[23] This alloy suffered from internal oxidation and chlorination along the grain boundaries as evidenced by Fig. 9. Alloys containing either Pd or Pt (Figs. 10 and 11) showed external iron and aluminium oxides, which have been dissolved by chlorides but in a much lower extent than the base $Fe_3Al$ alloy, showing the protective character of the corrosion products, explaining the lower corrosion rate of these alloys as shown in Figs. 1–10. Thus, it can be seen that the corrosion protection of an alloy against salt melt attack depends on the chemical stability of both kinds of metal and their compounds such as oxides and chlorides. In fact, a breakdown of the protective oxide readily occurs by dissolution into the melt, and the degradation rate can be especially fast if the oxide has a high solubility in

the melt. Since from a thermodynamic point of view, Al is the most reactive element among all the different investigated elements here, Al chloride or oxide forms preferentially over the other elements. At the melt/substrate interface, the oxygen potential is low while the chlorine potential is relatively high and, consequently, liquid aluminium chloride forms there and transports outwards, leaving an aluminium depleted layer as observed in Figs. 7–11. Near the melt/atmosphere interface, the transition from aluminium chloride to its oxide occurs, wherein only relatively low oxygen needs pressure because of the very stable nature of aluminium oxide. Therefore, the preferential removal of aluminium from the matrix is enhanced, basically in the form of highly volatile liquid chloride. This process seems to be beneficial to help establish a protective alumina, $Al_2O_3$, scale due to a fast aluminium supply. The role of the different alloying noble elements is to help to make more stable the alumina layer on top of the alloy and increase the alloy corrosion rate in the melt. In general, it has been shown that the presence of these noble elements decreases the $Fe_3Al$ alloy corrosion resistance at short times, but after a period of time, the formed corrosion products become more protective and the corrosion resistance of base $Fe_3Al$ alloy in molten NaCl–KCl is improved.

## Conclusions

A study on the effect of the addition of noble elements (Ag, AU, Pd and Pt) to an $Fe_3Al$ intermetallic alloy in its corrosion behaviour in molten NaCl–KCl at 700°C has been carried out using potentiodynamic polarisation curves, LPR and EIS. For comparison, the same tests were performed with commercial Ni based alloy Inconel 600. All the alloys showed an active behaviour without evidence of a passive layer. All different techniques showed that for short testing time, i.e. <40 h, the addition of these noble elements, except Au, decreased the corrosion rate of $Fe_3Al$ alloy, showing even higher corrosion rates than Inconel 600. However, for longer testing times, the addition of these noble elements improved the corrosion rate of unalloyed $Fe_3Al$ intermetallic alloy, showing corrosion rates lower than Ni based Inconel 600 alloy. The alloy containing Au showed the most stable corrosion rate values, whereas the one containing Ag suffered from localised corrosion around Ag particles.

## References


1. J. Klöwer: Proc. 2nd Int. Conf. on 'Heat-resistant materials', Gatlinburg, TN, USA, September 1995, ASM International, 245–252.
2. A. Nishikata and S. Haruyama: 'Electrochemical monitoring of the corrosion of Ni, Fe, and their alloys in molten salts', *Corrosion*, 1986, **42**, (10), 576–584.
3. P. F. Tortorelli and K. Natesan: 'Critical factors affecting the high-temperature corrosion performance of iron aluminides', *Mater. Sci. Eng. A*, 1998, **A258**, 115–125.
4. C. S. Ni, L. Y. Lu, C. L. Zeng and Y. Niu: 'Electrochemical impedance studies of the initial-stage corrosion of 310S stainless steel beneath thin film of molten $(0{\cdot}62Li, 0{\cdot}38K)_2CO_3$ at 650°C', *Corros. Sci.*, 2011, **53**, (3), 1018–1024.
5. Y. S. Li, M. Spiegel and S. Shimada: 'Corrosion behavior of various model alloys with NaCl–KCl coating', *Mater. Chem. Phys.*, 2005, **93**, (1), 217–223.
6. J. Lehmusto, B. J. Skrifvars, P. Yrjas and M. Hupa: 'High temperature oxidation of metallic chromium exposed to eight different metal chlorides', *Corros. Sci.*, 2011, **53**, 3315–3323.
7. M. Broström, S. Enestam, R. Backman and K. Mäkelä: 'Condensation in the KCl–NaCl system', *Fuel Process. Technol.*, 2013, **105**, 142–148.
8. M. Fukumoto, C. Tachikawame, Y. Matsuzaka and M. Hara: 'Formation of Si diffusion layer on stainless steels and their high temperature corrosion resistance in molten salt', *Corros. Sci.*, 2012, **56**, 105–113.
9. M. Ueda, H. Kigawa and T. Ohtsuka: 'Co-deposition of Al–Cr–Ni alloys using constant potential and potential pulse techniques in $AlCl_3$–NaCl–KCl molten salt', *Electrochim. Acta*, 2007, **52**, 2515–2519.
10. L. Zhang, X. Yu, Y. Dong, Z. Zhao, E. Chen and H. Liang: 'Preparation and properties of Al–Mn alloy coatings in NaCl–KCl–$AlCl_3$–$CeCl_3$ molten salts', *J. Rare Earths*, 2012, **30**, 278–282.
11. S.-H. Cho, J.-M. Hur, C.-S. Seo, J.-S. Yoon and S.-W. Park: 'Hot corrosion behavior of Ni-base alloys in a molten salt under an oxidizing atmosphere', *J. Alloys Compd*, 2009, **468**, 263–269.
12. N. N. Aung and X. Liu: 'High temperature electrochemical sensor for in situ monitoring of hot corrosion', *Corros. Sci.*, 2012, **12**, 1–4.
13. B. Zhu, G. Lindbergh and D. Simonsson: 'Comparison of electrochemical and surface characterisation methods for investigation of corrosion of bipolar plate materials in molten carbonate fuel cell: part I. Electrochemical study', *Corros. Sci.*, 1999, **41**, 1497–1513.
14. C. L. Zeng, W. Wang and W. T. Wu: 'Electrochemical-impedance study of the corrosion of Ni and FeAl intermetallic alloy in molten $(0{\cdot}62Li, 0{\cdot}38K)_2CO_3$ at 650°C', *Oxid. Met.*, 2000, **53**, 289–293.
15. C. Cuevas-Arteaga, J. Uruchurtu-Chavarin, J. G. Gonzalez, G. Izquierdo-Montalvo, J. Porcayo-Calderon and U. Cano: 'Corrosion evaluation of Incoloy 800 in sulfate/vanadate molten salts', *Corrosion*, 2004, **60**, 520–527.
16. U. Ducati, G. Lecis Coccia and G. Caironi: 'Electrochemical evaluation of hot corrosion resistance of metallic materials', *Mater. Chem. Phys.*, 1983, **8**, 135–145.
17. C. L. Zeng, P. Y. Guo and W. T. Wu: 'Electrochemical impedance spectra for the corrosion of two-phase Cu–15Al alloy in eutectic $(Li, K)_2CO_3$ at 650°C in air', *Electrochim. Acta*, 2004, **49**, 1445–1450.
18. C. L. Zeng, W. Wang and W. T. Wu: 'Electrochemical impedance models for molten salt corrosion', *Corros. Sci.*, 2001, **43**, 787–801.
19. J. I. Barraza-Fierro, M. A. Espinosa-Medina, M. Hernandez-Hernandez, H. B. Liu and E. Sosa-Hernandez: 'Effect of Li and Cu addition on corrosion of Fe–40 at.% Al intermetallics in molten LiCl–KCl eutectic salt', *Corros. Sci.*, 2012, **59**, 119–126.
20. S. I. Maldonado-Ruiz, D. Lopez, A. Velazco and R. Colas: 'Microstructural evaluation of wear resistant high chromium, high carbon cast irons', *Mater. Sci. Technol.*, 2004, **20**, 393–398.
21. J. G. Gonzalez-Rodriguez, O. L. Arenas, J. Porcayo-Calderon, V. M. Salinas-Bravo, M. Casales and A. Martinez-Villafañe: 'An electrochemical study of the effect of B on the corrosion of atomised Fe40Al intermetallics in molten $Na_2SO_4$', *High Temp. Mater. Processes*, 2006, **25**, 293–301.
22. P. Peled and D. Itzhak: 'The effect of noble alloying elements Ag, Pt and Au on the corrosion behavior of sintered stainless steel in an $H_2SO_4$ environment', *Corros. Sci.*, 1988, **28**, 1019–1028.
23. P. Peled and D. Itzhak: 'The surface composition of sintered stainless steel containing noble alloying elements exposed to a $H_2SO_4$ environment', *Corros. Sci.*, 1991, **32**, 83–90.
24. G. J. Janz, A. Conte and E. Neuenschwander: 'Corrosion of platinum, gold, silver and refractories in molten carbonates', *Corrosion*, 1963, **19**, 2921–2941.
25. G. J. Janz and A. Conte: 'Corrosion of gold–palladium, nickel and type 347 stainless steel in molten carbonates', *Corrosion*, 1964, **20**, 237t–238t.
26. Y. Niu, Z. L. Zhao, F. Gesmundo and M. Al-Omary: 'The air oxidation of two Cu–Ni–Ag alloys at 600–700°C', *Corros. Sci.*, 2001, **43**, 1541–1556.
27. X. X. Ma, Y. D. He and D. R. Wang: 'Inert anode composed of Ni–Cr alloy substrate, intermediate oxide film and $\alpha$-$Al_2O_3$/Au (Au–Pt, Au–Pd, Au–Rh) surface composite coating for aluminium electrolysis', *Corros. Sci.*, 2011, **53**, 1009–1017.
28. G. Wang, R. Carter and D. L. Douglass: 'High temperature sulfidation of Fe–Nb alloys', *Oxid. Met.*, 1989, **32**, 273–294.
29. R. Shiring and D. L. Douglass: 'Sulfidation behavior of rhenium and cobalt–rhenium alloys', *Oxid. Met.*, 1999, **52**, 353–377.